MATERIALE PLASTICE
https://revmaterialeplastice.ro
https://doi.org/10.37358/Mat.Plast.1964

Effect of 1,4-Naphthalenedicarboxylic Acid Derivative on Crystallization and Performances of Poly(L-lactide)

LISHA ZHAO[1], JUN QIAO[1], XUELING SHAN[1,2], YANHUA CAI[1,2*], JIE ZHANG[1]
[1]Chongqing Key Laboratory of Environmental Materials & Remediation Technologies, College of Chemistry and Environmental Engineering, Chongqing University of Arts and Sciences, Chongqing-402160, P.R. China
[2]School of Petrochemical Engineering, Changzhou University, Changzhou, Jiangsu-213164, P.R. China

Abstract: *In this work, biodegradable Poly(L-lactide) (PLLA) was modified through adding a new organic additive N, N'-bis(benzoyl) 1, 4-naphthalenedicarboxylic acid dihydrazide (NABH). A comparison on crystallization of the pure PLLA and PLLA/NABH revealed that the NABH as effective heterogeneous nucleation sites enhanced PLLA's crystallization, and an increase of NABH loading was able to further accelerate crystallization rate of PLLA; whereas a faster cooling rate was not conducive to PLLA's crystallization, but the appearance of obvious crystallization peak upon cooling at 30ºC/min confirmed the advanced enhancing role of NABH for PLLA crystallization again. The investigation on influence of the final melting temperature on the crystallization behavior of PLLA showed that the 170 ºC was optimum final melting temperature for enhancing crystallization, even the onset crystallization temperature of PLLA/NABH were higher than 150ºC. The melting processes of PLLA/NABH after different crystallization not only could reflect the previous crystallization, but also depended on crystallization temperature and heating rate. Thermal decomposition results showed that the existence of NABH slightly weakened thermal stability of PLLA, and the maximum difference in onset thermal decomposition temperature was only 9.4ºC comparing with the pure PLLA. However, the presence of NABH in PLLA matrix seriously weakened optical property.*

Keywords: *poly(L-lactide), benzoic hydrazide, nucleation effect, melt-crystallization, thermal stability*

1.Introduction

Solid waste pollution from the fossil-based and non-degradable polymeric products has led to a severe crisis for promoting social sustainable development, what is worse, up to now, the large-scale usage of non-degradable polymeric products has not been still reduced. Inevitably, developing bio-based and degradable polymeric materials as fossil-based polymers substitutions has become an important researching hotspot [1]. Poly(L-lactide) (PLLA) produced from renewable sources is widely known as a commercially available thermoplastic [2] with excellent degradability and compatibility [3, 4], easy processing [1, 5], appropriate mechanical performances [6, 7], etc. These advantages endow PLLA with promising applications in different fields, mostly for packaging materials [8-10], biomedical materials [11-13] and 3D printing materials [14-16]. For instance, to develop degradable carrier for controlled drug delivery, Li *et al* [17] prepared the polylactic acid composite membranes containing zeolitic imidazolate framework-8 *via* secondary growth method, the relative results indicated that the zeolitic imidazolate framework-8/polylactic acid composite membranes possessed excellent drug release and *p*H response capacity, and over 90% of loaded drug could be released in the buffer of *p*H value of 7.4.

However, the inherent drawbacks of high cost, slow crystallization rate, poor heat resistance and low crystallinity [2,18] seriously restrict the practical demanding applications of PLLA. Among aforementioned drawbacks, both poor heat resistance and low crystallinity result from the slow crystallization rate, additionally, the slow crystallization rate also affects PLLA's mechanical properties *via* forming amorphous products with low strength and modulus as well as poor dimensional stability [6]. Therefore, accelerating crystallization of PLLA is extremely important to remedy the performance defects of PLLA and thoroughly realize the replacement of the conventional fossil-based thermoplastic. Adding physical nucleating agent is thought to be an easy industrialization way to accelerate crystalli-

**email: mci651@163.com*

zation rate of semi-crystalline polymers, which is also suitable for PLLA. In the early research, the crystallization accelerating agent for PLLA focused on the commercial nucleating agents for other polymers such as polypropylene and polyethylene, these typical additives included clay [19-21], ethylene bis stearamide [20], calcium carbonate [22, 23], etc. After that, with the in-depth research, more inorganic or organic compounds including commercial or newly-synthesized compounds were employed to estimate their roles in enhancing PLLA's crystallization, and the relative results showed that metal phosphonates [24,25], inorganic whiskers [26,27], nano-inorganic matter [28,29], benzhydrazide derivatives [30,31], sorbitol derivatives [32,33] and 1H-benzotriazole derivatives [34] were highly effective nucleating agents for crystallization.

Through analysis, it is found that, in comparison to inorganic nucleator, the organic nucleator has attracted increasing attentions due to the better compatibility with PLLA and flexible designability of molecular structure. However, it is still unclear which key organic groups can affect the crystallization nucleation effect according to a finite category and quantity of the current organic nucleating agents. Thus, in this work, a new organic compound named *N, N′*-bis(benzoyl) 1, 4-naphthalenedicarboxylic acid dihydrazide (NABH) was developed to estimate its influences on the crystallization process, melting process, thermal decomposition behavior and optical property of PLLA. This work will be helpful to enrich the amount of organic nucleating agent and explore nucleation mechanism according to the relative key structure.

2.Materials and methods

Materials and reagents

A commercial grade 4032D PLLA produced by Nature-Works LLC was adopted. All reagents used to synthesis NABH were required to be analytically pure and directly used as received without purification before usage; these relative reagents included 1, 4-naphthalenedicarboxylic acid, benzoic hydrazide, *N, N′*-dimethylformamide (DMF), thionyl chloride and pyridine.

Synthesis of NABH

The synthetic pathway of NABH is shown in Figure 1. A detailed synthetic route is following: 9 g 1, 4-naphthalenedicarboxylic acid and 1mL DMF as catalyst were added into a three-necked flask with 60 mL thionyl chloride, respectively. And then with increasing of temperature to 80ºC, the solid-state 1, 4-naphthalenedicarboxylic acid was gradually dissolved in thionyl chloride with stirring, the aforementioned mixed solution were stirred at 80°C for 36 h, after that, 1, 4-naphthalenedicarboxylic acid dichloride was obtained *via* vacuum distillation. The 1, 4-naphthalenedicarboxylic acid dichloride was subsequently added into a solution including 0.006 mol benzoic hydrazide, 100 mL DMF and 3 mL pyridine, the mixture was stirred at ice bath for 1.5 h, heated up to 60°C to keep stirring for 3 h, the resulting solution was poured into 300 mL distilled water, the crude product was obtained by filtration method, and the crude product was further washed by distilled water for three times to obtain the final white product NABH. Fourier Transform Infrared Spectrometer (FT-IR) υ: 3448.2 cm^{-1} (N-H stretching vibrations absorption), 3173.7 and 688.9 cm^{-1} (C–H stretching vibration and the out-of-plane bending vibration absorption), 1654.1 cm^{-1} (stretching vibration absorption of C=O of synthesized amide), 1630.4 cm^{-1} (stretching vibration absorption of C=O of benzoic hydrazide), 1597.3, 1575.4, 1496.3 and 1442.6 cm^{-1} (vibration absorption of C–C of benzene and naphthalene), 1473.6 cm^{-1} (C-N-H bending vibration absorption), 1351.1 cm^{-1} (the mixed absorption about stretching vibration of C–N and bending vibration of N–H), 870.1 and 829.5 cm^{-1} (out-of-plane bending vibration absorption of C-H of aromatic hydrocarbon), 710.0 cm^{-1} (N-H out-of-plane bending absorption); ^{1}H Nuclear Magnetic Resonance (^{1}H NMR) δ: ppm; 10.69 (s 1H, NH), 10.60 (s, 1H, NH), 8.49~8.51 (m, 1H, Py), 7.99~8.01 (d, 2H, Py), 7.54~7.76 (m, 5H, Ar).

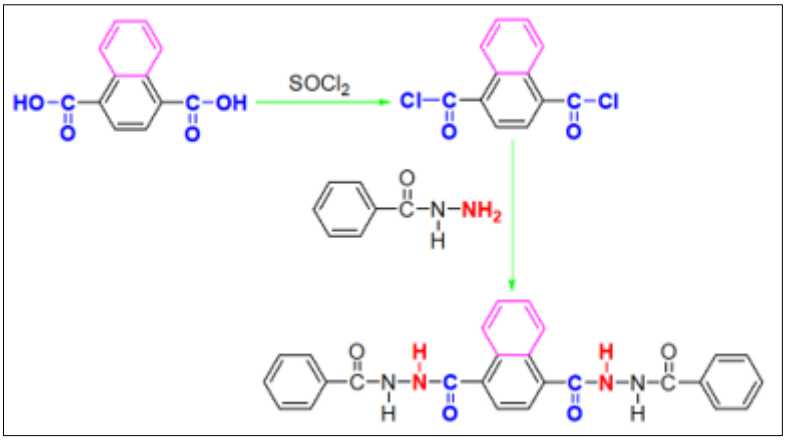

Figure 1. Synthetic pathway of NABH

Preparation of PLLA/NABH

First, PLLA and NABH were dried in vacuum at 45°C for 24 h to avoid the influence of water on the high temperature blending of PLLA with NABH. Second, The PLLA containing various NABH concentrations (0, 0.5, 1, 2 and 3 wt%) was blended on a torque rheometer, and the melt-blending temperature was set at 190°C; the blending rotation speed was set to be 32 rpm for 7 min, and then further increased to 64 rpm for 7 min. After that, the aforementioned mixture was hot pressed by 20 MPa pressure at 180°C, followed by cool-pressing at room temperature to obtain sample with a thickness of 0.4 mm to perform the relevant tests.

Test

Both crystallization and melting processes of the pure PLLA and modified PLLA were recorded by Q2000 DSC with 50 mL/min nitrogen. Although the testing conditions of crystallization and melting behaviors were different, the temperature and heat flow firstly needed to be calibrated using an indium standard before testing, and the thermal history also needed to be eliminated to ensure the relative tests at the same level. Under atmospheric condition, a Q500 TGA was used to perform a comparison test on thermal decomposition of the pure PLLA and modified PLLA, the testing temperature was from 40°C to 650°C with a heating rate of 5°C/min. The light transmittance was determined by the average value of the 5 times measurements using a DR82 transmittance instrument.

3.Results and discussions

Crystallization process

Upon cooling at 1 °C/min, the DSC thermograms of the pure PLLA and modified PLLA were displayed in Figure 2, and the relative crystallization parameters were listed in Table 1. As shown in Figure 2, DSC thermograms of the pure PLLA is clearly indicative of no melt-crystallization peak detected, indicating that, although that the cooling rate of 1°C/min is very slow, the pure PLLA cannot still form crystal in cooling *via* homogeneous nucleation, this finding confirms PLLA's poor crystallization ability as reported [35, 36]. In contrast with the pure PLLA, the melt-crystallization peaks of all PLLA/NABH samples can be easily detected in DSC thermograms, furthermore, the melt-crystallization peaks observed in DSC thermograms are very sharp, suggesting that the presence of NABH as effective heterogeneous nucleation sites is able to enhance crystallization ability and accelerate crystallization rate of PLLA. Additionally, Figure 2 displays the effect of NABH loading on the crystallization process of PLLA. Compared to the other three NABH loading, with the addition of 1 wt% NABH, the PLLA/1%NABH has the highest onset crystallization temperature (T_{oc}) of 142.3°C, crystallization peak temperature (T_{mc}) of 138.2°C, and the melting temperature (T_m) of 169.4°C, as well as the largest crystallization enthalpy (ΔH_c) of 48.9 J/g, showing that 1 wt% NABH is the optimal loading for inducing crystallization of PLLA. However, the temperature difference (ΔT_c) between T_{oc} and T_{mc} is

not the minimum value, which implies that the crystallization rate of PLLA/1%NABH is not the fastest in cooling, because a samller ΔT_c often means the faster crystallization rate. For the other three NABH loading of 0.5 wt%, 2 wt% and 3 wt%, an increase of NABH loading leads to a shift of crystallization peak to higher temperature side because of an increase of heterogeneous nucleation density in PLLA matrix; as seen in Table.1, the T_{oc} and T_{mc} increase from 137.7°C and 133.1°C to 139.4°C and 136.2°C, respectively; meanwhile the ΔT_c decreases from 4.6°C to 3.2°C, this drop in ΔT_c confirms that the NABH can accelerate PLLA's crystallization rate again. Overall, the addition of NABH can significantly promote the PLLA's crystallization in cooling, but the effect of NABH loading on the crystallization may depend not only on the NABH loading, but also the migration of PLLA chain segment.

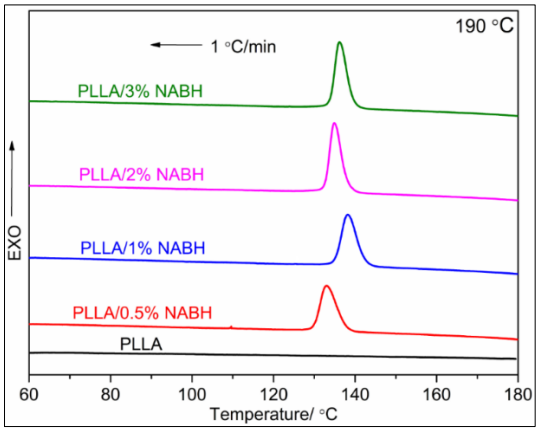

Figure 2. DSC thermograms of the pure PLLA and PLLA/NABH from the melt of 190°C at 1°C/min

Table 1. Crystallization DSC parameters of PLLA/NABH from the melt of 190 °C at 1°C/min

Sample	T_{oc} / °C	T_{mc} / °C	ΔT_c / °C	ΔH_c / J/g	T_m /°C
PLLA/0.5%NABH	137.7	133.1	4.6	48.3	168.0
PLLA/1%NABH	142.3	138.2	4.1	48.9	169.4
PLLA/2%NABH	138.1	134.9	3.2	48.4	168.4
PLLA/3%NABH	139.4	136.2	3.2	47.7	168.6

T_m: T_m was obtained during the second heating at a heating rate of 10°C/min

Evaluating crystallization ability of the modified PLLA at a higher cooling rate is necessary to practical production, because an increase of cooling rate often weakens the ability of additives for enhancing PLLA crystallization [37-39]. Figure 3 depicts the crystallization processes of PLLA/NABH from 190°C at various cooling rates (5, 10, 20 and 30°C/min). For a given PLLA/NABH sample, it is observed that a wider melt-crystallization peak located at lower temperature side appears in the DSC curve with an increase of cooling rate, suggesting a relative weaker crystallization ability and a relative slower crystallization rate. Even then, all PLLA/NABH still have obvious crystallization peaks at all cooing rates, even the NABH is still able to accelerate the PLLA's crystallization rate upon cooling at 30°C/min, which further confirms the advanced crystallization accelerating role of NABH. Additionally, upon cooling at a higher cooling rate, it is noteworthy that a larger NABH loading have a greater inhibition for preventing the weakness of crystallization ability as shown in Figure 3, the reason is that a larger amount of NABH can provide a higher nucleation density in PLLA matrix and cause melt-crystallization to occur at a relative higher temperature, which be proved by the crystallization peak shift toward higher temperature side with the increase in NABH loading in PLLA matrix.

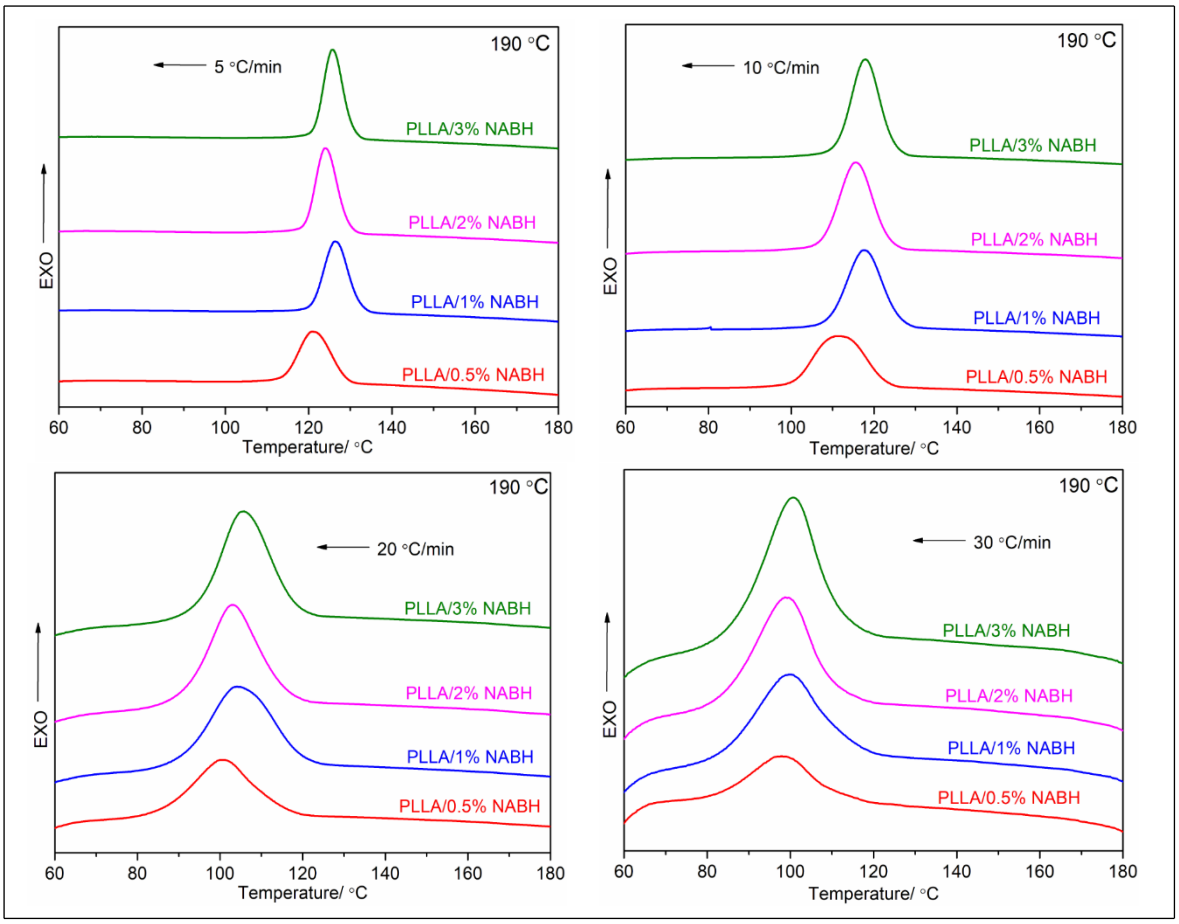

Figure 3. DSC thermograms of PLLA/NABH from 190°C at various cooling rates

The final melting temperature (T_f) determines solubility of NABH in PLLA resin according to the principle of "like dissolves like", correspondingly the T_f must affect the crystallization processes of PLLA/NABH in cooling. Figure 4 shows the DSC thermograms of PLLA/NABH from different T_f at a cooling rate of 1°C/min, and the relative crystallization parameters are listed in Table 2. As shown in Figure 4, the crystallization processes are significantly affected by T_f. When the T_f is 170°C, the crystallization peak moves toward the higher temperature side with the increase in NABH concentration, which is different from the results about the influence of NABH loading on the crystallization behaviors from other T_f at a cooling rate of 1°C/min. Moreover, Table.1 indicates that the T_f of 170°C is conducive to crystallize because of the presence of the highest T_{oc} and T_{mc} and the largest ΔH_c, the probable reason is that, on the hand, the relative low T_f in this study can provide the PLLA chain segment with excellent motility to ensure crystal growth; on the other hand, the relative low T_f can avoid the destruction of crystal stability resulting from the high temperature, as well as T_f of 170°C can ensure a larger amount of undissolved NABH as heterogeneous nucleus in PLLA matrix. Under this circumstance, PLLA/NABH have fast nucleation rate and crystal growth rate. As a result, the crystallization is completed in the higher temperature region. Additionally, it is noted that the T_{oc} of PLLA/2%NABH and PLLA/3%NABH are higher than 150°C, which is rather close to the melting range of the pure 4032D PLLA (about 160～175°C [40]), this result confirms the powerful crystallization ability of PLLA/NABH again. When the T_f is increased to 190°C, a given PLLA/NABH sample has the minimum T_{oc}, T_{mc} and ΔH_c, but the T_{oc}, T_{mc} and ΔH_c gradually increase when further increasing T_f to 200°C , this effect may depend on the interaction of PLLA with undissolved NABH, because an increase of T_f must dissolve more NABH in PLLA matrix, and these dissolved NABH can enhance the compatibility and interaction of PLLA with undissolved NABH, resulting in the fast and ordered arrangement of PLLA molecular chains.

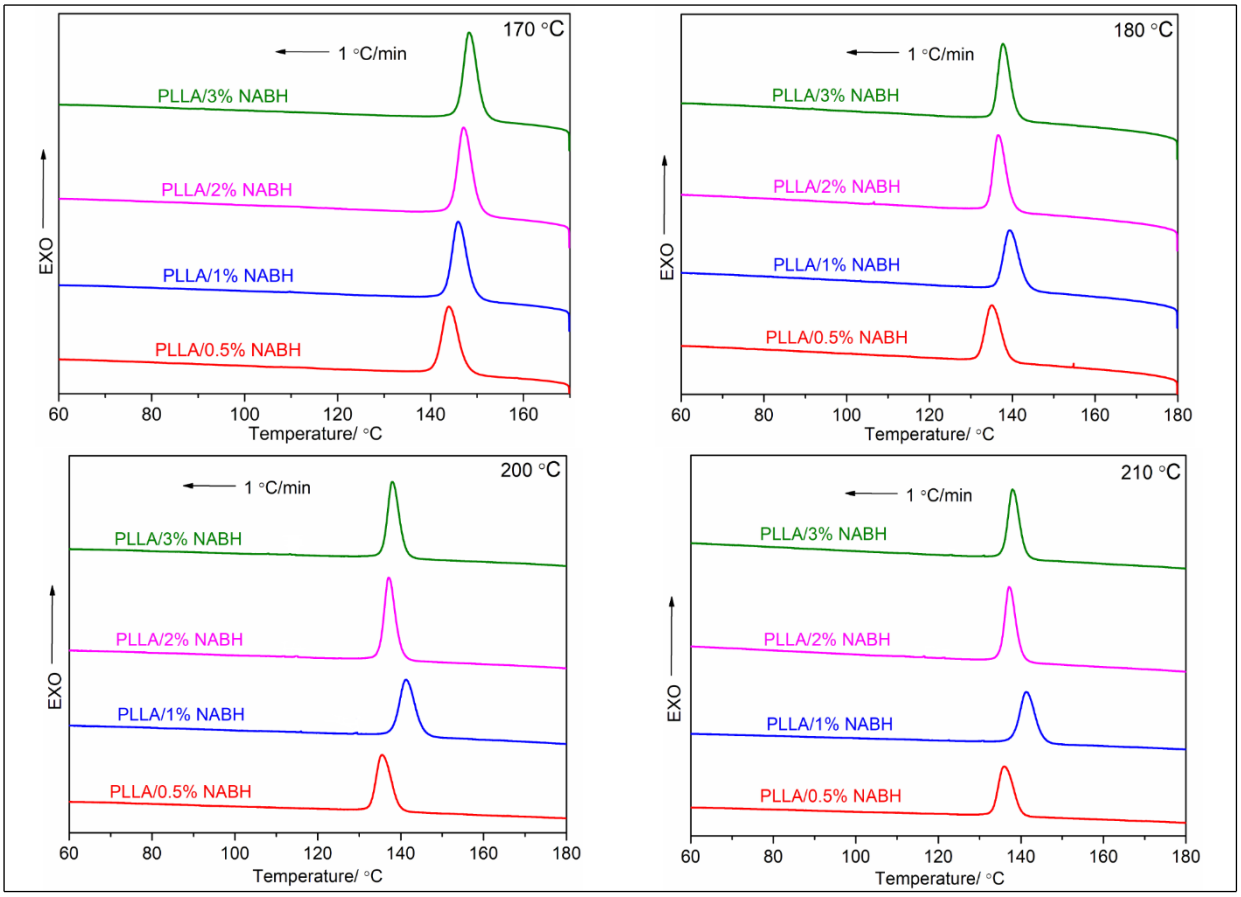

Figure 4. DSC thermograms of PLLA/NABH from various T_f at 1°C/min

Table 2. Crystallization DSC parameters of PLLA/NABH samples from various T_f at 1°C/min

T_f / °C	Sample	T_{oc} / °C	T_{mc} / °C	ΔT_c / °C	ΔH_c / J/g	T_m /°C
170	PLLA/0.5%NABH	147.8	144.0	3.8	54.7	171.2
	PLLA/1%NABH	149.5	145.9	3.6	55.4	171.9
	PLLA/2%NABH	150.5	147.1	3.4	55.1	172.1
	PLLA/3%NABH	151.5	148.3	3.2	53.5	172.3
180	PLLA/0.5%NABH	139.1	135.0	4.1	51.2	
	PLLA/1%NABH	143.6	139.4	4.2	52.3	169.5
	PLLA/2%NABH	140.1	136.6	3.5	50.3	168.7
	PLLA/3%NABH	141.1	137.7	3.4	52.2	168.8
200	PLLA/0.5%NABH	139.6	135.5	4.1	53.0	167.8
	PLLA/1%NABH	145.3	141.3	4.0	55.1	169.4
	PLLA/2%NABH	140.1	137.1	3.0	53.8	168.0
	PLLA/3%NABH	141.1	138.0	3.1	53.6	168.3
210	PLLA/0.5%NABH	140.0	136.0	4.0	54.0	167.9
	PLLA/1%NABH	145.2	141.3	3.9	55.2	169.0
	PLLA/2%NABH	140.1	137.2	2.9	55.5	167.8
	PLLA/3%NABH	141.0	138.0	3.0	53.7	168.1

Melting behavior

Usually, the melting behavior of semi-crystalline polymers depends on their crystallinity and crystal perfection. Figure 5 is DSC thermograms of PLLA/NABH at various heating rates (1, 2, 5 and 10°C/min) after melt-crystallization at 1°C/min. It can be observed from Figure 5 that, upon heating at 1°C/min, the PLLA/0.5%NABH has double melting peaks, the reason is that the rather slow heating rate of 1°C/min can further promote crystallization to occur, when the previous melt-crystallization cannot be thoroughly completed. However, it should be note that the high-temperature side melting peak is in the form of the shoulder peak, indicating that the amount of recrystallized crystals is very low. Upon heating at other rates, all PLLA/NABH only have the single melting peak, but the melting peak of a given PLLA/NABH becomes wider with an increase of heating rate due to the thermal hysteresis.

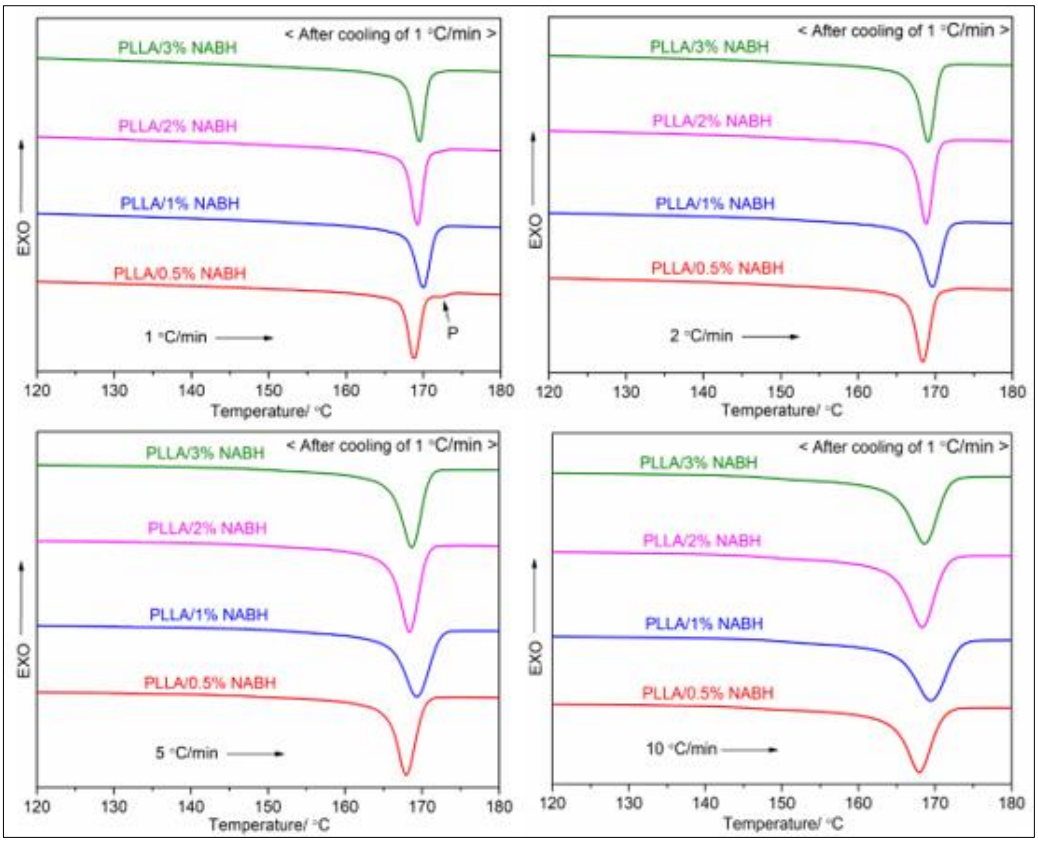

Figure 5. Melting behaviors of PLLA/NABH at various heating rates after melt-crystallization at 1 °C/min

In melt-crystallization section, the T_{mc} of all PLLA/NABH are about 130 °C～140°C, meaning the crystallization rate is the fastest in this temperature region. Thus, the melting behaviors of PLLA/NABH after isothermal crystallization in the temperature range of 130°C～140 °C were further studied by DSC, Figure.6 is the heating processes of PLLA/NABH at 10°C/min after isothermal crystallization at various crystallization temperatures (130, 132, 134, 136, 138 and 14°C) for 180 min. As isothermal crystallization temperature increases from 130°C to 140 °C, there are two typical features in DSC curves, one feature is that all PLLA/NABH exhibit the single melting peak, showing that the crystallization has been completed after sufficient crystallization for 180 min; another feature is that the single melting peak moves toward the higher temperature side with increasing of crystallization temperature, because a higher crystallization temperature can cause the crystal to grow more perfect.

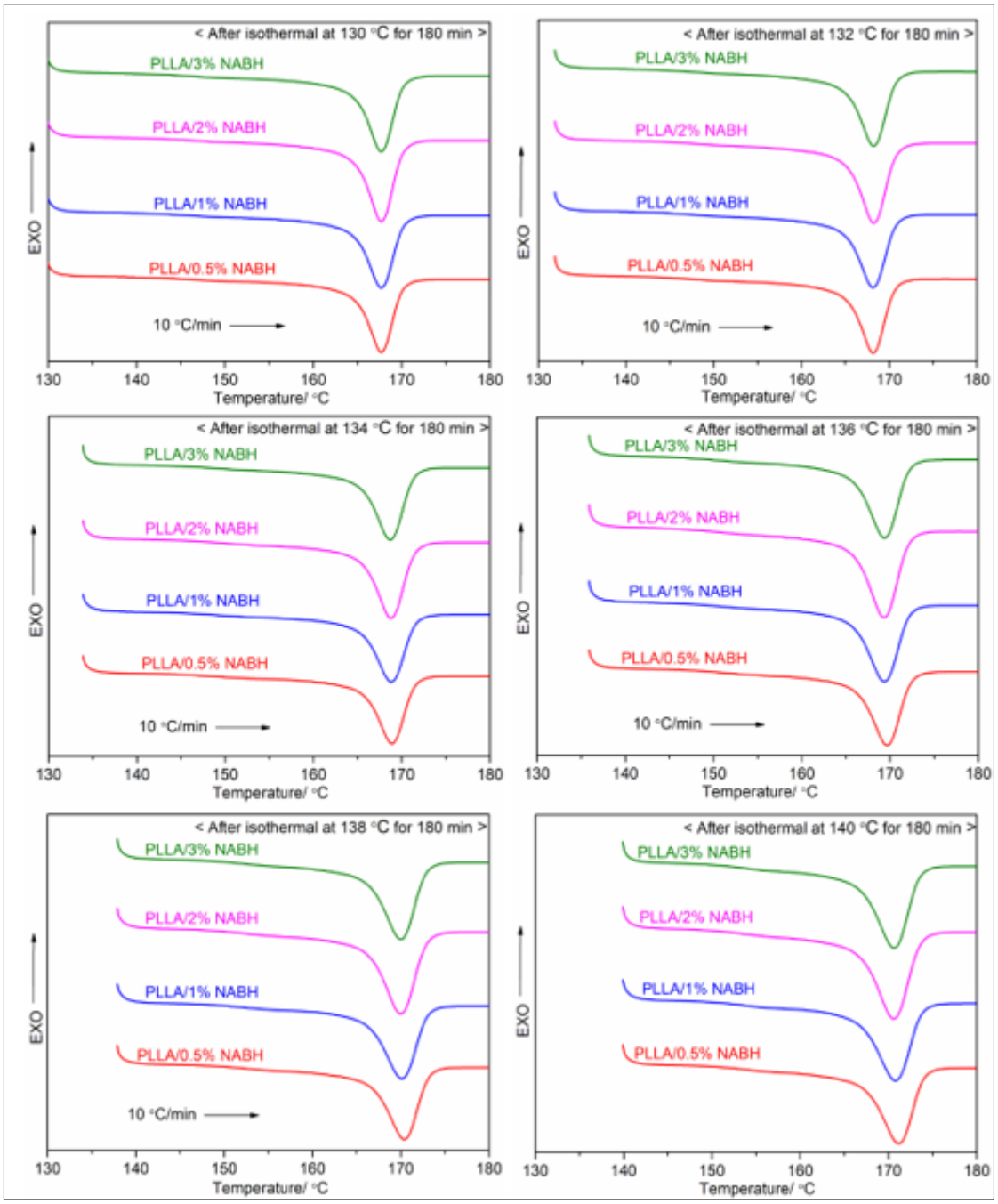

Figure 6. Melting behaviors of PLLA/NABH at the heating rate of 10°C/min after isothermal crystallization

Thermal stability and optical property

For practical application, investigating on the thermal decomposition behavior in air is very necessary to adapt for various applications. Hence, Figure 7 displays the TGA curves of the pure PLA and four PLA/NABH samples which exhibit only one mass loss stage of decomposition from TGA curves, and this mass loss stage appears in the temperature range of 300°C～400°C, which results from chain scissions and combustion of ester groups. Whereas the onset thermal decomposition temperature is affected by NABH, and the onset thermal decomposition temperatures are following: PLLA 341.3°C, PLLA/0.5%NABH 334.8°C, PLLA/1%NABH 334.4°C, PLLA/2%NABH 333.9°C and PLLA/3% NABH 331.9°C. Through data analysis, it is a fact that the presence of NABH weakens the thermal stability of PLLA, but there is no significant decrease, and the maximum difference in onset thermal

decomposition temperature is less than 10°C compared with the pure PLLA. Furthermore, although the onset thermal decomposition temperature decreases with increasing of NABH loading from 0.5 wt% to 3 wt%, the difference between all PLLA/NABH samples is only 2.9°C, indicating that the influence of NABH loading on the onset thermal decomposition temperature of PLLA/NABH is very slight.

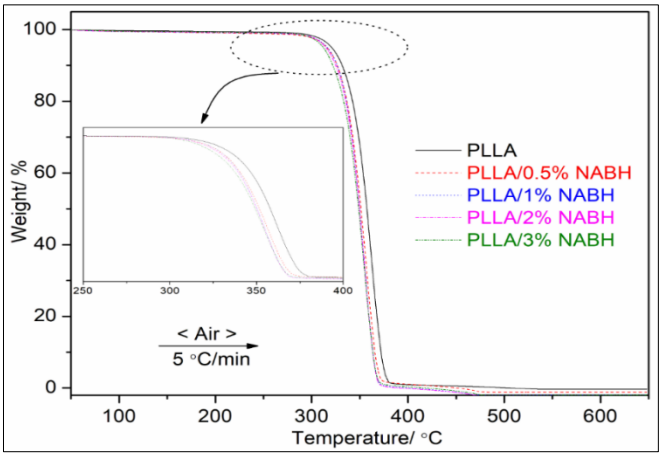

Figure 7. TGA curves of PLLA with and without NABH

Transparency is another important characteristic of PLLA itself, but the addition of a color additive often decreases the light transmittance, affecting its application in some fields. Figure 8 is the effect of NABH and its loading on PLLA's light transmittance, unfortunately, the introduction of NABH seriously destroys PLLA's light transmittance, when the NABH loading is 0.5 wt%, the light transmittance is decreased to 9.7% comparing with the 78.2% of the pure PLLA, what is worse, when the NABH loading is higher than 1 wt%, the light transmittance is almost zero, the primary reason is thought to be the white NABH in PLLA matrix. In addition, the crystallization promoting role of NABH can also make PLLA become opaque to some extent because of crystal formation.

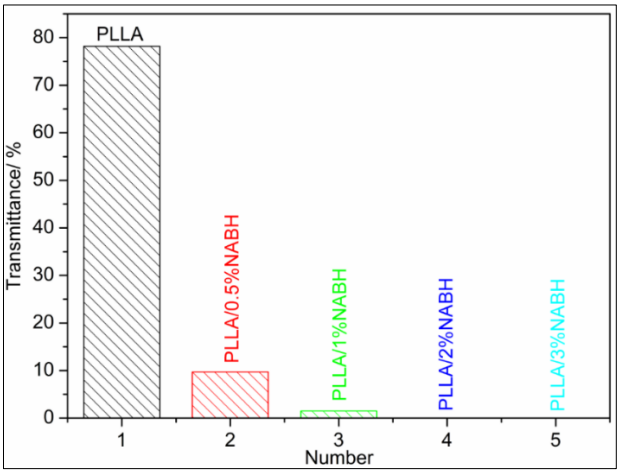

Figure 8 Light transmittance of the pure PLLA and PLLA/NABH

4.Conclusions

In conclusion, compared to the pure PLLA, the sharp crystallization peaks of all PLLA/NABH samples indicated that PLLA's crystallization ability was effectively improved by the introduction of NABH as a new organic heterogeneous nucleating agent. DSC measurements further showed that, upon cooling at 30ºC/min, PLLA/NABH could still crystallize resulting from the powerful promoting effect of NABH for PLLA's crystallization, although an increase of cooling rate was seriously negative to

PLLA/NABH's crystallization. Additionally, in melt-crystallization section, the influence of T_f on crystallization behavior showed that, when the T_f was 170ºC, PLLA/NABH exhibited the highest T_{oc}, T_{mc} and the largest ΔH_c. The heating rate significantly affected the melting behaviors of NABH-nucleated PLLA after melt-crystallization, and a decrease of heating rate could cause the melting peak to become sharper and promote the recrystallization to occur in heating. When the crystallization time was long enough, the melting behavior after isothermal crystallization depended on crystallization temperature. The incorporation of NABH could almost not change thermal decomposition profile of PLLA in air, moreover, the influence of NABH on the onset thermal decomposition temperature of PLLA was also not distinct, which is helpful to satisfy demanding applications. Unfortunately, the light transmittance of PLLA was seriously weakened by the NABH, when the NABH concentration was higher 1 wt%, the light transmission of PLLA/NABH was almost disappeared.

Acknowledgements: This study was supported by Foundation of Chongqing Science and Technology Bureau (cstc2019jcyj-msxmX0876) and Technological Research Program of Chongqing Municipal Education Commission (project number KJQN201801338).

References

1.CHEN P, ZHOU HF, LIU W, ZHANG M, DU ZJ, WANG XD. The synergistic effect of zinc oxide and phenylphosphonic acid zinc salt on the crystallization behavior of poly (lactic acid) [J], Polymer Degradation and Stability, 2015, 122: 25-35
2.PETCHWATTANA N, NAKNAEN P, NARUPAI B. Combination effects of reinforcing filler and impact modifier on the crystallization and toughening performances of poly(lactic acid) [J], Express Polymer Letters, 2020, 14(9): 848-859
3.FARIA ED, DIAS ML, FERREIRA LM, TAVARES MIB. Crystallization behavior of zinc oxide/poly(lactic acid) nanocomposites [J], Journal of Thermal Analysis and Calorimetry, 2020, DOI: 10.1007/s10973-020-10166-3
4.ZHEN ZY, XING Q, LI RB, DONG X. Crystallization behavior of polylactide nucleated by octamethylenedicarboxylic di(2-hydroxybenzohydrazide): Solubility influence [J], Thermochimica Acta, 2020, 683: 178447
5. XUE B, HE HZ, HUANG ZX, ZHU ZW, LI JQ, ZHAN ZM, CHEN M, WANG GZ, XIONG CT. Morphology evolution of poly(lactic acid) during in situ reaction with poly(butylenesuccinate) and ethylene-methyl acrylate-glycidyl methacrylate: The formation of a novel 3D star-like structure [J], Journal of Applied Polymer Science, 2020, 137(40): e49201
6. FOGLIA F, DE MEO A, IOZZINO V, VOLPE V, PANTANI R. Isothermal crystallization ofPLA: Nucleation density and growth rates of alpha and alpha' phases [J], Canadian Journal of Chemical Engineering, 2020, 98: 1998-2007
7. SOMSUNAN R, MAINOIY N. Isothermal and non-isothermal crystallization kinetics of PLA/PBS blends with talc as nucleating agent [J], Journal of Thermal Analysis and Calorimetry, 2020, 139(3): 1941-1948
8. NIKVARZ N, KHAYATI GR, SHARAFI S. Preparation of UV absorbent films using polylactic acid and grape syrup for food packaging application [J], Materials Letters, 2020, 276: 128187
9. GONZALEZ EAS, OLMOS D, LORENTE MA, VELAZ I, Gonzalez-Benito J. Preparation and characterization of polymer composite materials based on PLA/TiO_2 for antibacterial packaging [J], Polymers, 2018, 10(12): 1365
10. MULLER J, GONZALEZ-MARTINEZ C, CHIRALT A. Combination of poly(lactic) acid and starch for biodegradable food packaging [J], Materials, 2017, 10(8): 952
11. HUANG QL, LIU YS, OUYANG ZX, FENG QL. Comparing the regeneration potential between PLLA/Aragonite and PLLA/Vaterite pearl composite scaffolds in rabbit radius segmental bone defects [J], Bioactive Materials, 2020, 5(4): 980-989

12. RAMOS M, BELTRAN A, FORTUNATI E, PELTZER M, CRISTOFARO F, Visai L, VALENTE AJM, JIMENEZ A, KENNY JM, GARRIGOS MC. Controlled release of thymol from poly(lactic acid)-based silver nanocomposite films with antibacterial and antioxidant activity [J], Antioxidants, 2020, 9(5): 395
13.YANG FH, NIU XF, GU XN, XU CP, WANG W, FAN YB. Biodegradable magnesium-incorporated poly(L-lactic acid) microspheres for manipulation of drug release and alleviation of inflammatory response [J], ACS Applied Materials & Interfaces, 2019, 11(26): 23546-23557
14. MARCONI PL, TRENTINI A, ZAWOZNIK M, NADRA C, MERCADE JM, NOVOA JGS, OROZCO D, GROPPA MD. Development and testing of a 3D-printable polylactic acid device to optimize a water bioremediation process [J], AMB Express, 2020, 10(1): 142
15. ZHANG HG, ZHONG WU, HU QX, ABURAIA M, GONZALEZ-GUTIERREZ J, LAMMER H. Research and implementation of axial 3D printing method for PLA pipes [J], Applied Science-Basel, 2020, 10(13): 4680
16]. LIAO JJ, BROSSE N, PIZZI A, HOPPE S, ZHOU XJ, DU GB. Characterization and 3D printability of poly (lactic acid)/acetylated tannin composites [J], Industrial Crops and Products, 2020, 149: 112320
17. LIU WL, ZHANG H, ZHANG W, WANG M, LI JH, ZHANG Y, LI HY. Surface modification of a polylactic acid nanofiber membrane by zeolitic imidazolate framework-8 from secondary growth for drug delivery [J], Journal of Materials Science, 2020, 55(31): 15275-15287
18]. HUERTA-CARDOSO O, DURAZO-CARDENAS I, LONGHURST P, SIMMS NJ, ENCINAS-OROPESA A. Fabrication of agave tequilana bagasse/PLA composite and preliminary mechanical properties assessment [J], Industrial Crops and Products, 2020, 152: 112523
19. LI HB, HUNEAULT MA. Effect of nucleation and plasticization on the crystallization of poly(lactic acid) [J], Polymer, 2007, 48(23): 6855-6866
20. HARRIS AM, LEE EC. Improving mechanical performance of injection molded PLA by controlling crystallinity [J], Journal of Applied Polymer Science, 2008, 107(4): 2246-2255
21. DAY M, NAWABY AV, LIAO X. A DSC study of the crystallization behaviour of polylactic acid and its nanocomposites [J], Journal of Thermal Analysis and Calorimetry, 2006, 86(3): 623-629
22. SUKSUT B, DEEPRASERTKUL C. Effect of nucleating agents on physical properties of poly(lactic acid) and its blend with natural rubber [J], Journal of Polymers and the Environment, 2011, 19(1): 288-296
23. ZOU GX, ZHANG X, LI BJ, ZHAO CX, LI JC. Effect of mineral fillers on crystallization and melting behavior of poly(lactid acid)/mineral filler composites [J], Acta Polymerica Sinica, 2012, 9: 952-957
24. WANG SS, HAN CY, BIAN JJ, HAN LJ, WANG XM, DONG LS. Morphology, crystallization and enzymatic hydrolysis of poly(L-lactide) nucleated using layeredmetal phosphonates [J], Polymer Interantional, 2011, 60: 284-295
25. CAI YH, ZHAO LS. Magnesium phenylphosphonate: A additive for poly(L-lactic acid) [J], Materials Research Express, 2017, 4(3): 035305
26. ZHAO Y, LIU B, YOU C, CHEN MF. Effects of MgO whiskers on mechanical properties and crystallization behavior of PLLA/MgO composites [J], Materials and Design, 2016, 89: 573-581
27. CHEN RY, ZOU W, WU CR, JIA SK, HUANG Z, ZHANG GZ, YANG ZT. Poly(lactic acid)/poly(butylene succinate)/calcium sulfate whiskers biodegradable blends prepared by vane extruder: Analysis of mechanical properties, morphology, and crystallization behavior [J], Polymer Testing, 2014, 34: 1-9
28. SONG P, CHEN GY, WEI ZY, CHANG Y, ZHANG WX, LIANG JC. Rapid crystallization of poly(L-lactic acid) induced by a nanoscaled zinc citrate complex as nucleating agent [J], Polymer, 2012, 53(19): 4300-4309
29. GONG XH, PAN L, TANG CY, CHEN L, LI CQ, WU CG, LAW WC, WANG XT, TSUI CP, XIE XL. Investigating the crystallization behavior of poly(lactic acid) using CdSe/ZnS quantum dots as heterogeneous nucleating agents [J], Composites Part B-Engineering, 2016, 91: 103-110

30. KAWAMOTO N, SAKAI A, HORIKOSHI T, URUSHIHARA T, TOBITA E. Physical and mechanical properties of poly(L-lactic acid) nucleated by dibenzoylhydrazide compound [J], Journal of Applied Polymer Science, 2007, 103(1): 244-250
31. ZOU GX, JIAO QW, ZHANG X, ZHAO CX, LI JC. Crystallization behavior and morphology of poly(lactic acid) with a novel nucleating agent [J], Journal of Applied Polymer Science, 2015, 132(5): 41367
32. LAI WC, LIAO JP. Nucleation and crystal growth kinetics of poly(L-lactic acid) with self-assembled DBS nanofibrils [J], Materials Chemistry and Physics, 2013, 139(1): 161-168
33. YOU JX, YU W, ZHOU CX. Accelerated crystallization of poly(lactic acid): Synergistic effect of poly(ethylene glycol), dibenzylidene sorbitol, and long-chain branching [J], Industrial & Engineering Chemistry Research, 2014, 53(3): 1097-1107
34. ZHAO LS, CAI YH. A 1H-benzotriazole derivative nucleated poly(L-lactic acid): Thermal behavior and physical properties [J], Journal of the Chemical Society of Pakistan, 2020, 42(3): 383-389
35. CAI YH, TANG Y, ZHAO LS. Poly(L-lactic acid) with organic nucleating agent *N, N, N'*-tris(1H-benzotriazole) trimesinic acid acethydrazide: Crystallization and melting behavior [J], Journal of Applied Polymer Science, 2015, 132(32): 42402
36. FAN YQ, ZHU J, YAN SF, CHEN XS, YIN JB. Nucleating effect and crystal morphology controlling based on binary phase behavior between organic nucleating agent and poly(L-lactic acid) [J], Polymer, 2015, 67: 63-71
37. ZHAO LS, CAI YH, LIU HL. Physical properties of poly(L-lactic acid) fabricated using salicylic hydrazide derivative with tetraamide structure [J], Polymer-Plastics Technology and Materials, 2020, 59(2): 117-129
38. SU ZZ, GUO WH, LIU YJ, LI QY, WU CF. Non-isothermal crystallization kinetics of poly(lactic acid)/modified carbon black composite [J], Polymer Bulletin, 2009, 62: 629-642
39. CAI YH, ZHAO LS. Investigating on the modification of *N, N'*-adipic bis(benzoic acid) dihydrazide on poly (L-lactic acid) [J], Polymer Bulletin, 2019, 76(5): 2295-2310
40. WU T, TONG YR, QIU F, YUAN D, ZHANG GZ, QU JP. Morphology, rheology property, and crystallization behavior of PLLA/OMMT nanocomposites prepared by an innovative eccentric rotor extruder [J], Polymers for Advanced Technologies, 2018, 29(1): 41-51

Manuscript received: 23.11.2020